Probing the extent of the Sr^{2+} ion condensation to anionic polyacrylate coils: A quantitative anomalous small-angle x-ray scattering study

G. Goerigk, K. Huber, and R. Schweins

Citation: The Journal of Chemical Physics **127**, 154908 (2007); doi: 10.1063/1.2787008
View online: https://doi.org/10.1063/1.2787008
View Table of Contents: http://aip.scitation.org/toc/jcp/127/15
Published by the American Institute of Physics

Probing the extent of the Sr^{2+} ion condensation to anionic polyacrylate coils: A quantitative anomalous small-angle x-ray scattering study

G. Goerigk[a)]
Institut für Festkörperforschung, Forschungszentrum Jülich, Postfach 1913, D-52425 Jülich, Federal Republic of Germany

K. Huber
Department Chemie, Fakultät für Naturwissenschaften, Universität Paderborn, Warburgerstr. 100, D-33098 Paderborn, Federal Republic of Germany

R. Schweins
Large Scale Structures Group, Institut Laue-Langevin, 6 rue Jules Horowitz, B.P. 156, F-38042 Grenoble CEDEX 9 France

(Received 29 June 2007; accepted 28 August 2007; published online 18 October 2007)

The shrinking process of anionic sodium polyacrylate (NaPA) chains in aqueous solution induced by Sr^{2+} counterions was analyzed by anomalous small-angle x-ray scattering. Scattering experiments were performed close to the precipitation threshold of strontium polyacrylate. The pure-resonant scattering contribution, which is related to the structural distribution of the Sr^{2+} counterions, was used to analyze the extent of Sr^{2+} condensation onto the polyacrylate coils. A series of four samples with different ratios $[Sr^{2+}]/[NaPA]$ (between 0.451 and 0.464) has been investigated. From the quantitative analysis of the resonant invariant, the amount of Sr cations localized in the collapsed phase was calculated with concentrations $\bar{v}$ between 0.94×10^{17} and 2.01×10^{17} cm^{-3} corresponding to an amount of Sr cations in the collapsed phase between 9% and 23% of the total Sr^{2+} cations in solution. If compared to the concentration of polyacrylate expressed in moles of monomers [NaPA], a degree of site binding of $r=[Sr^{2+}]/[NaPA]$ between 0.05 and 0.11 was estimated. These values clearly differ from $r=0.25$, which was established from former light scattering experiments, indicating that the counterion condensation starts before the phase border is reached and increases rather sharply at the border. © *2007 American Institute of Physics*.
[DOI: 10.1063/1.2787008]

I. INTRODUCTION

The density of charges along a polyelectrolyte chain makes the chain conformation sensitive to electric charges. The two most efficient techniques to control changes in polyelectrolyte conformation are (i) the screening of electrostatic interactions among charged polymer segments by adding an inert salt[1] and (ii) the extinction of charges on the polyelectrolyte chain by adding specifically interacting counterions.[2,3] Synthetic polyelectrolytes may therefore be used as simple models for biopolymers, where the role of electric charges is essential for the proper functioning of nucleic acids, numerous enzymes, and proteins.

Theoretical understanding of the mechanism underlying the first technique has made significant progress. With increasing electrostatic screening, the shape of the polyelectrolyte gradually changes from a coil to a compact sphere, passing a cascade of transition states. For these transition states, cigarlike or pearl necklace structures are discussed. The latter were predicted in analogy to the Rayleigh instability of oil droplets while being electrically charged.[4,5] Beyond all doubt, the actual shape depends in a subtle way on the counterion concentration and interactions between solvent and chain backbone.[4–10] Although, the pearl necklace model has attracted much attention,[11–15] a quantitative analysis of the condensed phase is still lacking.

The present investigation focuses on the behavior of sodium polyacrylate (NaPA) chains, subjected to the addition of alkaline earth cations as an example for technique (ii). Alkaline earth cations are known to specifically interact with the anionic carboxylate residues, located on every other carbon atom of the polymer backbone. Formation of complex bonds between the anionic groups and alkaline earth cations neutralizes electric charges and thereby changes the nature of the respective chain segments. As a consequence, solubility of the polyelectrolyte is lowered, which leads to a significant coil shrinking and eventually causes a precipitation of the respective alkaline earth salt.[2,3,14,15]

The precipitation depends on the concentration of NaPA and of the alkaline earth cations, denoted as M^{2+}. Beyond a threshold concentration $[M^{2+}]_0$, an additional stoichiometric amount of M^{2+} per NaPA function is required to precipitate the polycarboxylate chains. This correlation can be represented in a phase diagram by means of a linear relation of the form $[M^{2+}]_c=[M^{2+}]_0+r_0[NaPA]_c$ which separates the one phase regime of a dilute solution from the precipitate, thus

a)Author to whom correspondence should be addressed. Also at JCNS-FRMII, c/o Technische Universität München, Lichtenbergstr. 1, D-85747 Garching, Federal Republic of Germany. Tel: +49-89-28910746. Fax: +49-89-28910798. Electronic mail: g.goerigk@fz-juelich.de.

acting as a phase boundary.[3,14] Based on light scattering measurements, changes in coil shape and size are expected to be more pronounced the closer one gets to this phase boundary. Although the coils adopt a spherelike shape prior to precipitation,[14] the shape of intermediates along the coil-to-sphere transition and especially the extent of M^{2+} condensation close to the phase border is still an unsettled question.

In this presentation, the question of how to determine the amount of Sr cations localized in the collapsed phase with respect to the total amount of Sr cations in the solvent, by precise analysis of what will be introduced below as the resonant invariant, while approaching the phase boundary of strontium polyacrylate (i.e., $M^{2+}=Sr^{2+}$) shall be addressed.

Anomalous small-angle x-ray scattering enables the quantitative and structural characterization of the counterion distribution around the macroions by tuning the energy in the vicinity of the absorption edge of the counterion (i.e., Sr^{2+}) in question. The distribution of the counterions is not accessible by conventional small-angle x-ray scattering measurements because the scattering contributions of the counterions and the macroions superimpose and cannot be distinguished. The first anomalous small-angle x-ray scattering (ASAXS) experiment on counterion distributions was reported by Stuhrmann.[16] Interest in the application of this promising method to macromolecules only revived at the turn of the century, propelled by the synthesis of new model polyelectrolytes.[17–21]

II. ASAXS MEASUREMENTS

In the case of a dilute solution of negatively charged polymers, which are surrounded by positively charged Sr counterions, the scattering amplitude writes

$$A(\mathbf{q}) = \int_V \Delta\rho_{\mathrm{poly}}(\mathbf{r}) \cdot \exp(-i\mathbf{qr}) d^3r + \int_V \Delta\rho_{\mathrm{Sr}}(\mathbf{r}) \cdot \exp(-i\mathbf{qr}) d^3r. \quad (1)$$

q is the magnitude of the scattering vector $[=(4\pi/\lambda)\sin\Theta]$, where 2Θ is the scattering angle and λ the x-ray wavelength. $\Delta\rho_{\mathrm{poly}}$ and $\Delta\rho_{\mathrm{Sr}}$ are the excess electron densities of the polyelectrolyte chains and the counterions,

$$\Delta\rho_{\mathrm{poly}}(\mathbf{r}) = \Delta f_{\mathrm{poly}} \cdot u(\mathbf{r}) = (f_{\mathrm{poly}} - \rho_m V_{\mathrm{poly}}) \cdot u(\mathbf{r}),$$

$$\Delta\rho_{\mathrm{Sr}}(\mathbf{r},E) = \Delta f_{\mathrm{Sr}}(E) \cdot v(\mathbf{r}) = ((f_{0,\mathrm{Sr}} - \rho_m V_{\mathrm{Sr}}) + f'_{\mathrm{Sr}}(E) + i f''_{\mathrm{Sr}}(E)) \cdot v(\mathbf{r}), \quad (2)$$

calculated from the electron density ρ_m of the solvent and the volume of the chain V_{poly} and the Sr^{2+} ion V_{Sr}, respectively, while $u(\mathbf{r})$ and $v(\mathbf{r})$ are the particle densities of the polymer chains and the Sr^{2+} ions, respectively. The molecular scattering factor (number of electrons) of the chain $f_{\mathrm{poly}}(E) \approx \mathrm{const}$ is nearly energy independent, while the atomic scattering factor of the counterions $f_{\mathrm{Sr}}(E)=f_{0,\mathrm{Sr}}+f'_{\mathrm{Sr}}(E)+if''_{\mathrm{Sr}}(E)$ shows strong energy dependent variation in the vicinity of the absorption edge of the Sr^{2+} ion due to the so-called anomalous dispersion corrections, $f'_{\mathrm{Sr}}(E)$ and $f''_{\mathrm{Sr}}(E)$. Calculating the scattering intensity $I(\mathbf{q})=|A(\mathbf{q})|^2=A(\mathbf{q})\cdot A^*(\mathbf{q})$ by means of Eqs. (1) and (2) and averaging over all orientations of the polymer yields a sum of three contributions $I(q,E) = |A_{\mathrm{poly}}(q)|^2 + 2\,\mathrm{Re}\,A_{\mathrm{poly}}(q)\,\mathrm{Re}\,A_{\mathrm{Sr}}(q,E) + |A_{\mathrm{Sr}}(q,E)|^2$, with the integrals[16]

$$|A_{\mathrm{poly}}(q)|^2 = 4\pi\Delta f_{\mathrm{poly}}^2 \int_V \int u(\mathbf{r})u(\mathbf{r}') \frac{\sin(q|\mathbf{r}-\mathbf{r}'|)}{q|\mathbf{r}-\mathbf{r}'|} d^3r d^3r',$$

$$2\,\mathrm{Re}\,A_{\mathrm{poly}}(q)\mathrm{Re}\,A_{\mathrm{Sr}}(q,E) = 4\pi 2\Delta f_{\mathrm{poly}}(f_{0,\mathrm{Sr}} - \rho_m V_{\mathrm{Sr}} + f'_{\mathrm{Sr}}(E)) \int_V \int u(\mathbf{r})v(\mathbf{r}') \frac{\sin(q|\mathbf{r}-\mathbf{r}'|)}{q|\mathbf{r}-\mathbf{r}'|} d^3r d^3r',$$

$$|A_{\mathrm{Sr}}(q,E)|^2 = 4\pi|\Delta f_{\mathrm{Sr}}(E)|^2 \int_V \int v(\mathbf{r})v(\mathbf{r}') \frac{\sin(q|\mathbf{r}-\mathbf{r}'|)}{q|\mathbf{r}-\mathbf{r}'|} d^3r d^3r'. \quad (3)$$

Equation (3) gives the nonresonant scattering of the polymer chains $|A_{\mathrm{poly}}(q)|^2$, the cross-term or mixed-resonant scattering $2\,\mathrm{Re}\,A_{\mathrm{poly}}(q)\,\mathrm{Re}\,A_{\mathrm{Sr}}(q,E)$ originating from the superposition of the scattering amplitudes of the polymer and the Sr^{2+} ions, and the scattering of the counterions $|A_{\mathrm{Sr}}(q,E)|^2$, which contains the so-called pure-resonant scattering. By measuring the scattering curves at two energies in the vicinity of the absorption edge of the Sr^{2+} ions and subtracting the two scattering curves $\Delta I(q,E_1,E_2)=I(q,E_1)-I(q,E_2)$, the nonresonant scattering contribution of the polymer is vanishing:

$$\Delta I(q,E_1,E_2) = 4\pi 2\Delta f_{\mathrm{poly}}(f'_{\mathrm{Sr}}(E_1) - f'_{\mathrm{Sr}}(E_2)) \int_V \int u(\mathbf{r})v(\mathbf{r}') \times \frac{\sin(q|\mathbf{r}-\mathbf{r}'|)}{q|\mathbf{r}-\mathbf{r}'|} d^3r d^3r' + 4\pi(|\Delta f_{\mathrm{Sr}}(E_1)|^2 - |\Delta f_{\mathrm{Sr}}(E_2)|^2) \int_V \int v(\mathbf{r})v(\mathbf{r}') \times \frac{\sin(q|\mathbf{r}-\mathbf{r}'|)}{q|\mathbf{r}-\mathbf{r}'|} d^3r d^3r'. \quad (4)$$

Now the scattering function is reduced to the resonant contributions—the so-called separated scattering—but the scattering of the polymer is still present in the cross-term. The significance of this term was outlined by Jusufi and Ballauff, who were able to demonstrate that it may lead directly to the Fourier transform of the density distribution of the polyelectrolyte component if the polyelectrolyte component is a rigid colloid.[22,23] However, additional knowledge of the third integral in Eq. (3) is required. One route to determine the third integral is to perform measurement at a third energy. When subtracting the separated scattering curves obtained at the two energies E_1 and E_3 from the separated scattering obtained from the two energies E_1 and E_2, the cross-term is vanishing and the form factor $S_{\mathrm{Sr}}^{\mathrm{form}}(q)$ of the spatial

distribution of the Sr^{2+} ions remains after normalizing to the energy dependent anomalous dispersion corrections of the atomic scattering factor of the Sr^{2+} ions at the related energies:

$$S_{\mathrm{Sr}}^{\mathrm{form}}(q) = 4\pi \int_V \int v(\mathbf{r}) v(\mathbf{r}') \frac{\sin(q|\mathbf{r}-\mathbf{r}'|)}{q|\mathbf{r}-\mathbf{r}'|} d^3r d^3r'$$
$$= \left[\frac{\Delta I_0(q,E_1,E_2)}{f'_{\mathrm{Sr}}(E_1) - f'_{\mathrm{Sr}}(E_2)} - \frac{\Delta I_0(q,E_1,E_3)}{f'_{\mathrm{Sr}}(E_1) - f'_{\mathrm{Sr}}(E_3)} \right] \frac{1}{F(E_1,E_2,E_3)},$$

$$F(E_1,E_2,E_3) = f'_{\mathrm{Sr}}(E_2) - f'_{\mathrm{Sr}}(E_3) + \frac{f''^2_{\mathrm{Sr}}(E_1) - f''^2_{\mathrm{Sr}}(E_2)}{f'_{\mathrm{Sr}}(E_1) - f'_{\mathrm{Sr}}(E_2)} - \frac{f''^2_{\mathrm{Sr}}(E_1) - f''^2_{\mathrm{Sr}}(E_3)}{f'_{\mathrm{Sr}}(E_1) - f'_{\mathrm{Sr}}(E_3)}. \quad (5)$$

Due to Eq. (5), ASAXS provides a technique to access directly the scattering of the Sr^{2+} ions. The structural information of the Sr^{2+} ion distribution surrounding the macroions can be obtained from the analysis of the form factor $S_{\mathrm{Sr}}^{\mathrm{form}}(q)$. Generally speaking, Eq. (5) provides a method which gives access to the pure-resonant scattering contribution by measuring the small-angle scattering at only three suitable energies.[15,24,25] An alternative route to separate all three integrals was achieved by Ballauff and co-workers,[26,27] which could afford to record scattering curves at 4 (Ref. 26) and 13 (Ref. 27) different energies below the absorption edge of the fluctuating counterions. This enabled them to determine the three scattering contributions (nonresonant, mixed-resonant, and resonant terms) by means of a plot of $I(q,E)$ vs f'_{eff} and a fit with a sum of the integrals of Eq. (3) at variable q.

In addition to the structural information, which can be obtained from $S_{\mathrm{Sr}}^{\mathrm{form}}(q)$, important quantitative information related to the amount of Sr atoms localized in the collapsed phase can be deduced from the integral Q_{Sr}:

$$Q_{\mathrm{Sr}}(E) = \frac{1}{4\pi} \int_Q |A_{\mathrm{Sr}}(q,E)|^2 d^3q = \frac{1}{4\pi} |\Delta f_{\mathrm{Sr}}(E)|^2 \int_Q S_{\mathrm{Sr}}^{\mathrm{form}}(q) d^3q. \quad (6)$$

In analogy to the so-called invariant,[28] we will call Q_{Sr} the resonant invariant of the inhomogeneously distributed resonant scattering Sr ions. The invariant Q_{Sr}, as defined in Eq. (6), is related to the averaged squared excess electron density of the resonant scattering atoms,[28] $\overline{\eta_{\mathrm{Sr}}^2}$:

$$Q_{\mathrm{Sr}}(E) = (2\pi)^3 V \overline{\eta_{\mathrm{Sr}}^2(E)}. \quad (7)$$

where V is the sample volume. With the averaged squared excess electron density of the Sr ions, $\overline{\eta_{\mathrm{Sr}}^2(E)} = \overline{(\rho_{\mathrm{Sr}}(E) - \bar{\rho}_{\mathrm{Sr}}(E))^2} = \overline{\rho_{\mathrm{Sr}}^2(E)} - \overline{\rho_{\mathrm{Sr}}(E)^2}$, Eq. (7) writes

$$Q_{\mathrm{Sr}}(E) = (2\pi)^3 V (\overline{\rho_{\mathrm{Sr}}^2(E)} - \overline{\rho_{\mathrm{Sr}}(E)^2}). \quad (8)$$

Introducing $\rho_{\mathrm{Sr}}(\mathbf{r},E) = f_{\mathrm{Sr}}(E) v(\mathbf{r})$, which represents the electron density distribution of the Sr ions in the solution [Eq. (2)], into Eq. (8) yields

$$Q_{\mathrm{Sr}}(E) = (2\pi)^3 V |f_{\mathrm{Sr}}(E)|^2 (\overline{v^2} - \bar{v}^2). \quad (9)$$

For the subsequent calculations, the calibration of the scattering curves into macroscopic scattering cross sections in units of cross section per unit volume (cm^{-1}) is mandatory. To obtain the calibration, Eq. (9) must be multiplied with r_0^2/V, where r_0 is the classical electron radius:

$$Q_{\mathrm{Sr}}(E) = (2\pi)^3 r_0^2 |f_{\mathrm{Sr}}(E)|^2 (\overline{v^2} - \bar{v}^2). \quad (10)$$

Because only the excess electron density of the Sr ions with respect to the solvent contributes to the scattering, $f_{\mathrm{Sr}}(E)$ can be replaced by $\Delta f_{\mathrm{Sr}}(E)$ from Eq. (2):

$$Q_{\mathrm{Sr}}(E) = (2\pi)^3 r_0^2 |\Delta f_{\mathrm{Sr}}(E)|^2 (\overline{v^2} - \bar{v}^2). \quad (11)$$

The averaged squared number density of Sr ions can be written as

$$\overline{v^2} = \frac{N_{\mathrm{Sr}} V_{\mathrm{Sr}}}{V} \frac{1}{V_{\mathrm{Sr}}^2} = \frac{\bar{v}}{V_{\mathrm{Sr}}}, \quad (12)$$

where $V_{\mathrm{Sr}} = 4\pi/3 R_{\mathrm{Sr}}^3$ is the volume of a single Sr ion with the radius $R_{\mathrm{Sr}} = 0.126$ nm. N_{Sr} represents the total number of Sr ions in the solvent. Inserting Eq. (12) into Eq. (11) yields

$$Q_{\mathrm{Sr}}(E) = (2\pi)^3 r_0^2 |\Delta f_{\mathrm{Sr}}(E)|^2 \bar{v} \left(\frac{1}{V_{\mathrm{Sr}}} - \bar{v} \right) \approx (2\pi)^3 r_0^2 |\Delta f_{\mathrm{Sr}}(E)|^2 \frac{\bar{v}}{V_{\mathrm{Sr}}}. \quad (13)$$

Combining Eqs. (6) and (13) yields

$$Q_{\mathrm{Sr}}(E) = \frac{|\Delta f_{\mathrm{Sr}}(E)|^2}{4\pi} \int_Q S_{\mathrm{Sr}}^{\mathrm{form}}(q) d^3q \approx (2\pi)^3 r_0^2 |\Delta f_{\mathrm{Sr}}(E)|^2 \frac{\bar{v}}{V_{\mathrm{Sr}}}, \quad (14a)$$

$$\frac{dQ_{\mathrm{Sr}}(E)}{dq} = |\Delta f_{\mathrm{Sr}}(E)|^2 S_{\mathrm{Sr}}^{\mathrm{form}}(q) q^2. \quad (14b)$$

Equation (14b) represents the first derivative of the resonant invariant with respect to q and will be used in Fig. 3. Finally, from Eq. (14a) the number density of the Sr ions can be calculated:

$$\bar{v} = \frac{V_{\mathrm{Sr}} Q_{\mathrm{Sr}}}{(2\pi)^3 r_0^2 |\Delta f_{\mathrm{Sr}}(E)|^2}. \quad (15)$$

It should be mentioned that the number density calculated from Eq. (15) includes the Sr ions, which are homogeneously distributed in the solvent. These Sr ions provide an isotropic scattering contribution at small q values similar to the isotropic scattering of the solvent but with a different amount. As will be discussed in more detail below, the amount of the isotropic scattering contribution originating from these remaining Sr ions in the solvent can be neglected.

III. EXPERIMENTAL

Preparation of NaPA solutions with Sr^{2+} in aqueous NaCl was performed in two steps. In the first step, a solution of NaPA in bidistilled water with 0.01*M* NaCl at *p*H 9 (solution I) was prepared together with another solution of 3 mM $SrCl_2$ and 4 mM NaCl in bidistilled water at *p*H 9 (solution II). The *p*H was set with 0.01*M* NaOH. It is noteworthy to mention that both solutions had the same number of cationic charges, which was $2[Sr^{2+}]+[Na^+]=0.01M$. After 3 days of storage, equal volumes of both solutions were combined. Thus, a stock solution of NaPA in distilled water with 1.5 mM $SrCl_2$ and 7 mM NaCl with a *p*H of 9 was obtained (solution III). In an analogous way, an amount of solution II was combined with an equal amount of bidistilled water with 0.01*M* NaCl, resulting in a NaPA-free solution of 1.5 mM $SrCl_2$ and 7 mM NaCl at a *p*H of 9 (solution IV). Solution IV is denoted as solvent and served as the solvent background for all scattering experiments. The phase boundary for Sr^{2+}-PA precipitation was approached by diluting the stock solution (III) with the solvent (IV). By means of this procedure,[25] four different ratios of $[Sr^{2+}]/[NaPA]$ were obtained at constant concentrations of $[Sr^{2+}]$ and $[Na^+]$ ($[Sr^{2+}]/[NaPA]=0.451$, 0.4575, 0.458, and 0.464), denoted as samples D, C, B, and A, respectively. As the shape of the polymer chains in solution depends on the extent of complexation, different ratios correspond to different intermediates, bordering the precipitation threshold of SrPA.

Combined static and dynamic light scattering measurements (ALV 5000E CGS) allowed us to locate the precipitation threshold and to characterize the global dimensions of the polymer chains in dependence on the ratio of $[Sr^{2+}]/[NaPA]$.[25]

The four samples selected for ASAXS as well as the solvent were filled into capillaries from Hilgenberg GmbH, Malsfeld, Germany. The capillaries are made of borosilicate glass with an inner diameter of 4 mm and a wall thickness of 0.05 mm. The inner diameter of 4 mm is nearly the optimal size for the energy range of the Sr *K* edge at 16.105 keV. The capillaries were closed with a pipette plug fixed by two component quick setting adhesive.

ASAXS measurements were performed at the JUSIFA beamline[29] at HASYLAB, DESY Hamburg at three different energies in the energy range of the *K* absorption edge of strontium at 16.105 keV. Measurements were made with a two-dimensional detector at three energies. A q range from about 0.07 to 2.7 nm^{-1} was covered. A detailed description of the experiments can be found in Ref. 25.

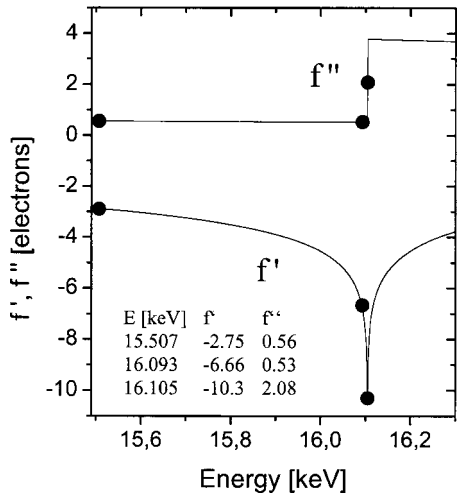

FIG. 1. Anomalous dispersion corrections obtained by Cromer-Liberman calculations (Refs. 30 and 31). The values at 16.105 keV result from the convolution with the energy resolution of the JUSIFA beamline.

The table in Fig. 1 provides the anomalous dispersion corrections for Sr at the three energies used here based on the calculations of Cromer and Liberman.[30,31] These were used to permit the separation of the Sr-related pure-resonant scattering described in detail by Eqs. (1)–(5). Constant background effects due to resonant raman scattering and fluorescence occurring near the *K* absorption edge at 16.105 keV have been subtracted from the measured intensities. The scattering intensity is calibrated into macroscopic scattering cross sections in units of cross section per unit volume ($cm^2/cm^3=cm^{-1}$). Transmission measurements were performed with a precision of 0.001 using a special (windowless) photodiode (Hamamatsu S2387-1010N). The amount of the integrated form factors [Eq. (5)] with respect to the integrated total scattering, i.e., $\varepsilon=\int S_{Sr}^{form}(q)d^3q/\int I(q,E)d^3q$, of the four samples was between 0.25% and 0.60% (last column in Table I).

TABLE I. Structural and quantitative parameters of the four diluted NaPA samples with different concentration ratios $[Sr^{2+}]/[NaPA]$ obtained from the ASAXS analysis. $\bar{v}$ represents the concentration of Sr atoms in the condensed phase deduced from the experimentally accessible section of resonant invariant. Values of $\bar{v}^u$ represent the upper limits of these concentrations calculated with the different theoretical model functions of the dumbbell (PD and PS+D). c is the relative amount of Sr atoms in the condensed phase with respect to the total concentration of Sr ions in the entire solution and r represents the ratio of Sr cations to carboxylate side groups in the collapsed phase. Sample A represents an outlier possibly due to degradation of the sample. The latter was evidenced by LS experiments showing strong differences of the radius of gyration taken before and after the ASAXS measurements (Ref. 25).

Sample	$[Sr^{2+}]/[NaPA]$	$\bar{v}$ (10^{17} cm^{-3})	$\bar{v}^u$ (PD) (10^{17} cm^{-3})	$\bar{v}^u$ (PS+D) (10^{17} cm^{-3})	c^a (%)	r	ε (%)
A	0.464	0.77(14)	0.94	1.17	10.5–13.1	0.049–0.061	0.30
B	0.458	1.50(8)	1.92	2.09	21.4–23.3	0.097–0.106	0.50
C	0.4575	1.73(21)	2.01	2.09	22.3–23.2	0.102–0.106	0.60
D	0.451	0.73(12)	0.80	⋯	8.9	0.041	0.25

[a]The values refers to 9.0×10^{17} Sr^{2+} cations per cm^3 which correspond to 1.5 mM.

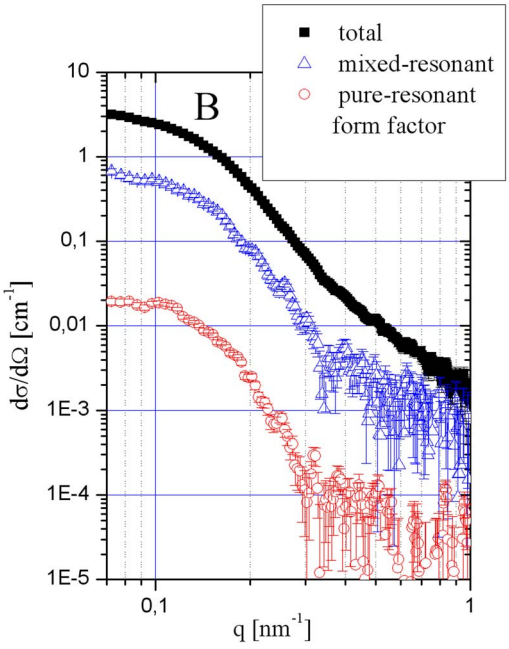

FIG. 2. (Color online) Total scattering (squares), separated scattering (triangles), and the form factor of the pure-resonant scattering contribution (circles) of the aqueous polyacrylate solution with Sr ions from sample B with a concentration ratio $[Sr^{2+}]/[NaPA]=0.458$.

IV. RESULTS AND DISCUSSION

The focus of the present work is the development of the resonant invariant of the Sr^{2+} ions. A detailed description of the scattering pattern is given only for sample B with $[Sr^{2+}]/[NaPA]=0.458$ in Fig. 2. The shape of the total scattering curve (black squares) is compatible with the form factor of spherical objects. The latter was already suggested by former small-angle neutron scattering measurements.[32] This interpretation is strongly confirmed by the separated scattering curve (blue triangles) and the separated form factor (red circles) of the Sr ion distribution. The error bars of the separated form factor were calculated from the error bars of the total scattering curves measured at the three energies considering the error propagation through Eq. (5). In the q range between 0.07 and 0.3 nm^{-1}, relative errors between 10% and 40% have been obtained. Both curves exhibit a number of characteristic structures for $q>0.1$ nm^{-1} with pronounced maxima, minima, and shoulders revealing a scattering function, which is strongly influenced by correlation effects between rather monodisperse subdomains within the collapsing chains. Especially, the form factors of the spatial distribution of the Sr counterions reveal a correlation maximum at 0.1 nm^{-1}. For a counterion condensation-induced shrinking process, an appropriate model was first suggested by Dobrynin *et al.*[5] which was confirmed later by computer simulations.[7,8,10] The model, denoted as pearl necklace, gives the scattering function of N spheres with radius R and with a distance d between the spheres.

Scattering data corresponding to the resonant scattering curves can also be represented by means of Eq. (14b). This representation is shown in Fig. 3 for all four samples. The area corresponding to these data represents the experimentally accessible portion of the invariant, denoted as $Q_{Sr}(exp)$.

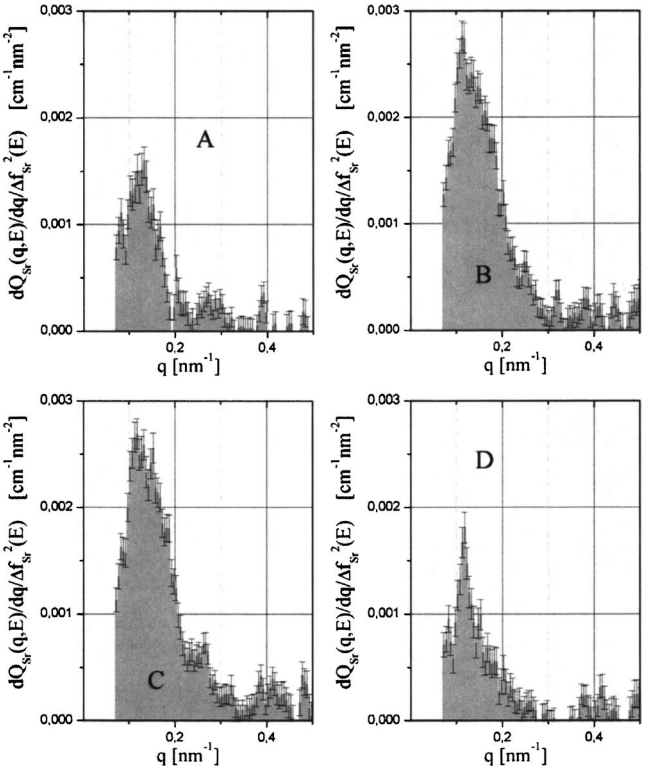

FIG. 3. The first derivative of the resonant invariant [Eq. (14b)] of the four samples [$[Sr^{2+}]/[NaPA]=0.451$ (D), 0.4575 (C), 0.458 (B), and 0.464 (A)].

Table I summarizes the concentrations $\bar{v}$ of Sr ions in the condensed phase obtained from this resonant invariant depicted with Eqs. (14b) and (15).

For a more quantitative discussion of the data, this limited area has to be extended onto the whole regime of $0 \leqslant q < \infty$. Estimation of the extensions (especially to very small q values, $q<0.075$ nm^{-1}) will be carried out by three sphere-based models being capable of reproducing the scattering data under consideration. It has to be emphasized that the major purpose of these model applications in the present case is to estimate the contribution of the low and high q regimes of the $S_{Sr}^{form}(q)$ to the resonant invariant of Eq. (15), determined experimentally.

Two models have already been applied to the same data in a preceding work.[25] The model consisting of a polydisperse sphere, denoted as the PS model, is the simplest model. It provided already a good representation of the data.[25] The PS model is based on a Schulz-Flory type of distribution $P(M)$ of the polymer mass M,[25,33]

$$P(M) = \left(\frac{z+1}{M_w}\right)^{z+1} \frac{M^z}{\Gamma(z+1)} \exp\left(-\frac{(z+1)M}{M_w}\right). \tag{16}$$

In Eq. (16), the polydispersity is fixed by $z=1/(M_w/M_n-1)$, with M_w and M_n the weight averaged and the number averaged mass of the spheres. However, the averaged particle size of this model was considerably smaller than the respective value established independently by light scattering. Hence, we added an appropriate portion of monodisperse dumbbells, which increased the average size of the model without significantly affecting the scattering curves at $q>0.1$ nm^{-1}. This second model is denoted as the PS+D

TABLE II. Model representations have been applied to the scattering curves obtained from ASAXS experiments in order to estimate the extension of these scattering curves beyond the limits accessible to the experiment. Representation with the PS model and the PS+D model was inferred from Ref. 25. Representation of the data with the PD model was performed by means of a least squares fit making use of Eq. (17). The symbols have the following meaning: The values for R_g in column 3 represent values for the radii of gyration of the polymer particles determined experimentally by light scattering. (Ref. 25). The PS model is a polydisperse sphere model where R_z denotes the z-averaged outer sphere radius. In the PS+D model, R_z, d, and R_D denote the z-averaged radius of the outer sphere radius of the sphere component, the distance between two spheres in the dumbbell component, and the outer sphere radius of the monodisperse spheres in the dumbbell component, respectively. In the PD model, R_z, d, and z denote the z-averaged radius of the outer sphere radius of the spheres in the dumbbells, the distance between two spheres in the dumbbell component, and the polydispersity parameter $z=1/(M_w/M_n-1)$ of the spheres of the dumbbell component, respectively. Model parameters of the models are applied to reproduce the resonant invariants in Fig. 3.

			PS model	PS+D model			PD model		
Sample	$[Sr^{2+}]/[NaPA]$	R_g[a] (nm)	R_z (nm)	R_z[a]	d	R_D	R_z	d	z
A	0.464	17.3	16	16	55	16	15	55	1.30
B	0.458	23.2	15	16	55	16	13	71	1.31
C	0.4575	21.3	15	16	55	16	13	56	1.42
D	0.451	30.7	15	16	55	16	14	67	1.13

[a]The sphere fraction is characterized by a polydispersity parameter of $z=5$.

model in what follows. In order to provide one more curve, which is easily accessible from a least squares fit to data, a third model will be introduced here. This model represents a pearl necklace with N identical spheres and a distribution of the sphere size according to the Schulz-Flory type of distribution. The sphere size is R and the distance between two neighboring spheres on a dumbbell is d.

In Eq. (17), the form factor of a sphere is multiplied with the correlations (first bracket) introduced by the interference of the scattering from the two spheres. Polydispersity of the pearls is considered by means of a Schulz-Flory type of distribution $P(M)$, again following Eq. (16).[25,33] The particle mass M in Eq. (17) is proportional to $2R^3$ and the polydispersity is fixed by $z=1/(M_w/M_n-1)$, with M_w and M_n the weight averaged and the number averaged mass of the dumbbells.

$$S_{\mathrm{Sr}}^{\mathrm{form}}(q) = \mathrm{const}\int_0^\infty P(M(R))\left(2+2\frac{\sin(qd)}{qd}\right) \times\left(\frac{4\pi R^3}{3}\frac{3(\sin(qR)-qR\cos(qR))}{(qR)^3}\right)^2 dR. \quad (17)$$

This PD model has to provide only an alternative estimation of the portion of the invariant not accessible to the ASAXS experiment. No further development of a structural concept of the collapsing PA coils which goes beyond the interpretation given in Ref. 25 is intended in the present work. Model parameters for all three models which succeeded to reproduce the experimentally determined resonant scattering curves are summarized in Table II.

From the resonant invariant in Figs. 3(a)–3(d), an amount between $0.73\times10^{17}<\bar{v}<1.73\times10^{17}$ Sr atoms per cm^3 was calculated to be in the condensed phase for the four samples (column 3 in Table I). An estimation of the amount of scattering contributions, which could not be detected due to the limited q resolution of the experiment, is outlined in Fig. 4 for sample B. The gray area represents this contribution of the anomalous small-angle x-ray scattering from the q range below the resolution of the experiment. It has been extrapolated from the different model functions as mentioned above. Above the resolution, we integrated up to $q=10\ \mathrm{nm}^{-1}$ obtaining additional contributions, which can be neglected with respect to the contributions of the gray area. Addition of the values from the gray area to the respective $\bar{v}$ values of column 3 derived from $Q_{\mathrm{Sr}}(\mathrm{exp})$ via Eq. (15) results in estimations of the Sr^{2+} concentrations shown in columns 4 and 5 of Table I. The numbers in columns 4 and 5 are considered to be upper limits for the Sr concentration in the collapsed phase suggested from the different models and are denoted $\bar{v}^u$. In addition, the inset of Fig. 4 represents the contribution of homogeneously distributed Sr ions with a concentration of 1.5 mM to the resonant invariant. Although this corresponds to the maximum possible amount—a considerable portion of the Sr^{2+} ions are condensed on the NaPA chains—the contribution is many orders of magnitude

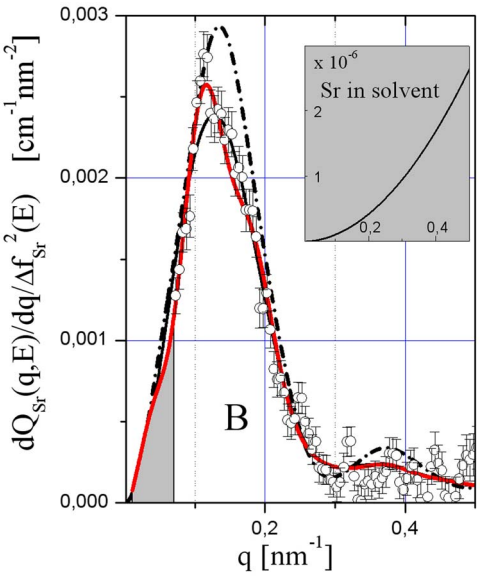

FIG. 4. (Color online) The first derivative of the resonant invariant [Eq. (14b)] of sample B compared to three different model functions, PD (solid red line), PS+D (black dashed line), and PS (black solid line). The different model functions were calculated in order to estimate the contribution of the missing scattering to the resonant invariant beyond the resolution of the ASAXS experiment (gray area on the left). The inset 4 represents the upper limit of the scattering from 1.5 mM of homogeneously distributed Sr ions in the solution, contributing to the resonant invariant.

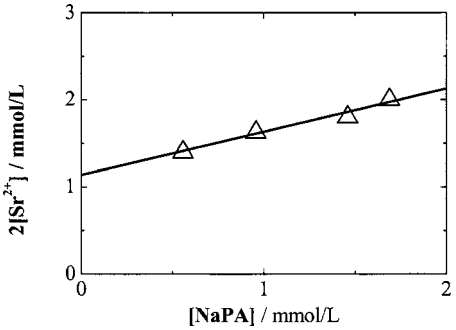

FIG. 5. Phase diagram established for SrPA precipitation in 0.01*M* NaCl (Ref. 25). The Sr^{2+}-counterion concentration is plotted vs the macroion (polyacrylate) concentration. The triangles correspond to results obtained from light scattering. The solid line represents the phase border between the collapsed and the noncollapsed polymer chains with a slope of $r=0.25$.

smaller than the contribution detected from the Sr ions in the collapsed phase and thus can be neglected. Hence, the resonant invariant estimated here can be attributed unambiguously to the condensed Sr^{2+} ions.

As inferred from the preparation, the concentration of Sr ions of 1.5 mM corresponds to $9\times10^{17}Sr^{2+}$ ions per cm^{-3}. Together with the concentration values $\bar{v}^u$ deduced from the resonant invariant, this led to a fraction of condensed Sr ions lying between 9% and 23% of the total Sr ions in the entire solution. From the concentrations of condensed Sr^{2+} ions, $\bar{v}^u$, the corresponding ratios, $r=[Sr^{2+}]/[NaPA]$, were calculated by taking into account the q regimes beyond the experimental cutoff. The values depend on the ratio of the component concentrations expressed as $[Sr^{2+}]/[NaPA]$ and fall in a regime of $0.05<0.11$ Sr ions, which are bound per carboxylate residue on the polymer backbone. This result can be compared to a value of $r=0.25$ extracted from the phase diagram in Fig. 5 established by Schweins *et al.*[25] The straight line in Fig. 5 represents the phase border between Sr-polyacrylate precipitates and the collapsed polymer or partially collapsed macroions in solution. The value of $r=0.25$ indicates the amount which is needed to cross the phase border along the collapsed state. For a quantitative discussion of the r values in Table I, sample A has to be considered with great care because light scattering of the samples performed prior to and after the ASAXS experiments indicated a slight instability.[25] Except for this sample A, the values of r follow our expectations. Samples B and C are close together and sample D shows a smaller degree of Sr^{2+} binding in line with a drop of $[Sr^{2+}]/[NaPA]$ from B/C to D. The drastic effect confirms that small changes in $[Sr^{2+}]/[NaPA]$ cause strong changes in the conformation and hence in r once we get close to the phase boundary, as has been already observed in our preceding experiment.[15] The closer the sample gets to the phase boundary, the higher the degree of Sr^{2+} binding becomes.

Noteworthy, Molnar and Rieger[34] published a molecular dynamics simulation[13] of the interaction of NaPA oligomers with Ca^{2+} cations. They found an abrupt increase of free Na^+ ions if more than three Ca^{2+} cations have been added to the "simulated cubic solution box." This supports the feature of a rather abrupt increase of the decoration of the PA coils with Sr^{2+} if the system gets close to the phase boundary.

The discrepancy between the value obtained from the phase diagram and the values deduced from the resonant invariant can be explained as follows: (i) There is an error of the slope due to the scattering of the points, which is fairly large. Beyond this, the exact location of the phase boundary may depend on the molar mass of the polyacrylate sample actually used.[2,14] (ii) At the phase border, an upper limit of Sr^{2+} ions is considered to be captured by the PA coils, while the Sr^{2+} condensation is a process gradually starting before the phase border is reached. Under the assumption that we have not yet reached the phase border with our samples B–D, the actual degree of Sr binding may still be considerably lower than the characteristic value at the phase boundary. Thus, the discrepancy between $r=0.11$ and $r=0.25$ corresponding to the phase boundary implies another steep increase of the bound Sr^{2+}, in agreement with the drastic changes observed at the precipitation edge.

The latter explanation demonstrates that precise quantitative ASAXS measurements employing the algorithm in Sec. II. with the goal to obtain the resonant invariant could serve as a suitable tool for detailed quantitative analysis of those phase diagrams in the future.

V. CONCLUSIONS

In the last years, anomalous small-angle x-ray scattering became a precise quantitative method for element specific structural analysis on the mesoscopic length scale. Due to the precision of the techniques, small-angle scattering contributions in the resolution regime $10^{-3}<\Delta I/I<10^{-2}$ can be reliably separated and the form factor of the pure-resonant scattering of counterion distributions around macroions becomes accessible, as was demonstrated for Sr-counterion-induced shrinking of polyacrylates.

The form factor of inhomogeneously distributed Sr counterions was separated with an amount between 0.3% and 0.6% with respect to the total scattering. The form factor is attributed to a collapsed phase in a diluted aqueous polyacrylate solution with the Sr counterions condensing in the collapsed phase. From the integral of the separated form factor (resonant invariant), different amounts between 9% and 23% of the Sr counterions were deduced as being captured in the collapsed phase. The numbers also indicate a sharp increase of Sr^{2+} binding close to the phase border established from light scattering (LS) measurements. The example demonstrates the capability to determine quantitatively the extent of ion binding to polyelectrolytes which condense to or interact specifically with the polyelectrolyte.

[1] M. Nagasawa, *Studies in Polymer Science* (Elsevier Science, Amsterdam, 1988), Vol. 2, p. 49.
[2] K. Huber, J. Phys. Chem. **97**, 9825 (1993).
[3] I. Michaeli, J. Polym. Sci. **48**, 291 (1960).
[4] Y. Kantor and M. Kardar, Europhys. Lett. **27**, 643 (1994).
[5] A. V. Dobrynin, M. Rubinstein, and S. P. Obukhov, Macromolecules **29**, 2974 (1996).
[6] F. J. Solis and M. Olvera de la Cruz, Macromolecules **31**, 5502 (1998).
[7] U. Micka, Ch. Holm, and K. Kremer, Langmuir **15**, 4033 (1999).
[8] P. Chodanowski and S. Stoll, J. Chem. Phys. **111**, 6069 (1999).
[9] A. V. Lyulin, B. Dünweg, O. V. Borisov, and A. A. Darinskii, Macromolecules **32**, 3264 (1999).
[10] H. J. Limbach and Ch. Holm, J. Phys. Chem. B **107**, 8041 (2003).

[11] V. O. Aseyev, S. I. Klenin, H. Tenhu, I. Grillo, and E. Geissler, Macromolecules **34**, 3706 (2001).
[12] M.-J. Li, M. M. Green, and H. Morawetz, Macromolecules **35**, 4216 (2002).
[13] S. Minko, A. Kiriy, G. Gorodyska, and M. Stamm, J. Am. Chem. Soc. **124**, 10192 (2002).
[14] R. Schweins and K. Huber, Eur. Phys. J. E **5**, 117 (2001).
[15] G. Goerigk, R. Schweins, K. Huber, and M. Ballauff, Europhys. Lett. **66**(3), 331 (2004).
[16] H. B. Stuhrmann, Adv. Polym. Sci. **67**, 123 (1985).
[17] Q. de Robilliard, X. Guo, N. Dingenouts, M. Ballauff, and G. Goerigk, Macromol. Symp. **164**, 81 (2001).
[18] B. Guilleaume, M. Ballauff, G. Goerigk, M. Wittemann, and M. Rehahn, Colloid Polym. Sci. **279**, 829 (2001).
[19] B. Guilleaume, J. Blaul, M. Ballauff, M. Wittemann, M. Rehahn, and G. Goerigk, Eur. Phys. J. E **8**, 299 (2002).
[20] I. Sabbagh, M. Delsanti, and P. Lesieur, Eur. Phys. J. B **12**, 253 (1999).
[21] R. Das, T. T. Mills, L. W. Kwok, G. S. Maskel, L. S. Millet, S. Doniach, K. D. Finkelstein, D. Herschlag, and L. Pollack, Phys. Rev. Lett. **90**, 188103 (2003).
[22] M. Ballauff and A. Jusufi, Colloid Polym. Sci. **284**, 1303 (2006).
[23] A. Jusufi and M. Ballauff, Macromol. Theory Simul. **15**, 193 (2006).
[24] G. Goerigk and D. L. Williamson, J. Appl. Phys. **99**, 084309 (2006).
[25] R. Schweins, G. Goerigk, and K. Huber, Eur. Phys. J. E **21**, 99 (2006).
[26] M. Patel, S. Rosenfeldt, N. Dingenouts, D. Pontoni, T. Narayanan, and M. Ballauff, Phys. Chem. Chem. Phys. **6**, 2962 (2004).
[27] N. Dingenouts, M. Patel, S. Rosenfeldt, D. Pontoni, T. Narayanan, and M. Ballauff, Macromolecules **37**, 8152 (2004).
[28] O. Glatter and O. Kratky, *Small-Angle X-ray Scattering* (Academic, London, 1982).
[29] H.-G. Haubold, K. Gruenhagen, M. Wagener, H. Jungbluth, H. Heer, A. Pfeil, H. Rongen, G. Brandenburg, R. Moeller, J. Matzerath, P. Hiller, and H. Halling, Rev. Sci. Instrum. **60**, 1943(1989).
[30] D. T. Cromer and D. Liberman, J. Chem. Phys. **53**, 1891 (1970).
[31] D. T. Cromer and D. Liberman, Acta Crystallogr., Sect. A: Cryst. Phys., Diffr., Theor. Gen. Crystallogr. **A37**, 267 (1981).
[32] R. Schweins, P. Lindner, and K. Huber, Macromolecules **36**, 9564 (2003).
[33] B. Zimm, J. Chem. Phys. **16**, 1099 (1978).
[34] F. Molnar and J. Rieger, Langmuir **21**, 786 (2005).